Original Article

Check for updates

Available online at
www.heca-analitika.com/hjas

Heca Journal of Applied Sciences

Vol. 4, No. 2, 2026

RE-PAD: A Modular Renewable-Powered Auxiliary System for Decoupling Radiator Cooling Fans in Isolated Diesel Power Plants

Marzuirman Marzuirman [1], Agus Rendi Wijaya [1], Ahmad Fachrurrozi [1], Ramadhan Farhan Fadillah [1], Derry Pradana Nasrul [1], Erkata Yandri [1,2,*], Ahmad Zulfikri Taning [1,2], and Aep Saepul Uyun [1,2]

1 Graduate School of Renewable Energy - Darma Persada University. Jl. Radin Inten 2. Pondok Kelapa. East Jakarta 13450, Indonesia; marzuirman@gmail.com (M.M.); agusrendiwijaya@gmail.com (A.R.W.); rozisontoloyo@gmail.com (A.F.); ramadhann.farhannn@gmail.com (R.F.F.); derrypradhanafisika@gmail.com (D.P.N.); erkata@gmail.com (E.Y.); ahmad.z.taning@gmail.com (A.Z.T.); aepsuyun@gmail.com (A.S.U.)

2 Center of Renewable Energy Studies, Darma Persada University, Jl. Radin Inten 2, Pondok Kelapa, East Jakarta 13450, Indonesia

* Correspondence: erkata@gmail.com

Article History

Received 4 July 2026
Revised 30 August 2026
Accepted 6 September 2026
Available Online 15 September 2026

Keywords:
Pahl and Beitz methodology
Pugh matrix
Parasitic load
B40 biodiesel
Variable frequency drive
Requirement traceability

Abstract

Engine-driven radiator cooling fans in isolated diesel power plants impose a continuous mechanical parasitic load typically reported at 3–7% of rated engine power, a burden compounded by Indonesia's B40 biodiesel mandate, which increases cooling-system heat-rejection demand, yet no study identified in the authors' prior systematic review documents a formal, traceable engineering design process for addressing this problem through auxiliary-load decoupling. This study aims to systematically elicit design requirements, generate and evaluate alternative technical concepts, and specify a traceable modular architecture for parasitic-load decoupling in a B40-fuelled isolated diesel generator. A systematic engineering design methodology, following the Pahl & Beitz/VDI 2221–2223 framework, was applied to the Caterpillar 3512B LY800217 (1024 kW) unit operated by PLN Nusa Daya in Kepulauan Riau, comprising requirement elicitation, functional decomposition, morphological analysis, and Pugh-based concept selection, with requirement coverage examined through a traceability matrix and the robustness of the concept ranking examined through a weighting sensitivity check. Six functional requirements yielded four concept variants; Pugh scoring, supported by the sensitivity analysis, indicated that a fully renewable-decoupled configuration (net score +5) was preferred over a hybrid renewable-with-fallback alternative (net score +3) under equal criterion weighting, principally through complete satisfaction of the parasitic-load-elimination requirement, with the ranking reversing only where retrofit capital cost is weighted dominantly. The selected six-module Renewable-Powered Auxiliary Decoupling (RE-PAD) architecture was shown, through traceability analysis, to conceptually address all elicited requirements without gap, and preliminary literature-based screening indicated technical plausibility relative to comparable variable-frequency-drive and biodiesel-thermal studies; the parasitic-load magnitude (estimated at 41.0 kW, 4.0% of rated output) and the component ratings presented remain preliminary values whose thermal and techno-economic validation is reported in a companion simulation study (in preparation). The architecture supports a conceptually scalable, phased retrofit pathway for the approximately 80-unit PLN Nusa Daya isolated diesel fleet, subject to per-unit sizing confirmation.

1. Introduction

Isolated diesel power plants (PLTDs) remain a principal source of electricity for remote islands and off-grid communities across archipelagic Indonesia, where geographic dispersion often precludes connection to the national interconnected grid [1, 2]. As of 2025, PT PLN (Persero) operates more than 5,000 diesel generator sets across eastern Indonesia, Nusa Tenggara, Maluku, Papua, and the Riau and Kepulauan Riau archipelagos, with a collective installed capacity exceeding 3,000 MW. Isolated diesel generation therefore remains a structurally important component of the national power system [2, 3]. These systems are characterized by relatively high specific fuel consumption, with fuel costs typically accounting for 60–70% of total operating expenditure, as well as logistical vulnerability associated with dependence on maritime fuel-supply chains to remote locations [4, 5].

In parallel, the Indonesian government has implemented a mandatory progressive biodiesel blending program, advancing from B20 in 2016 and B30 in 2020 to B40 in 2025 under Peraturan Menteri ESDM No. 12 Tahun 2023. The policy requires diesel fuel consumed nationally, including fuel used by isolated power plants, to contain at least 40% fatty acid methyl ester (FAME) derived from palm oil [6, 7]. The B40 mandate simultaneously pursues three national objectives: reducing dependence on imported fossil fuels, supporting the domestic palm-oil industry, and contributing to Indonesia's Nationally Determined Contribution target of a 29% reduction in greenhouse-gas emissions by 2030 [7]. However, this transition is not thermally neutral. High-concentration biodiesel blends can alter combustion behavior and engine heat-rejection characteristics, potentially increasing demands on cooling systems that, in many isolated PLTD units, have remained largely unchanged since commissioning.

Within the cooling system, the radiator fan represents a particularly consequential yet frequently overlooked auxiliary load. In many isolated PLTD units, the fan remains mechanically coupled to the engine crankshaft and therefore consumes power continuously irrespective of actual thermal demand. This parasitic consumption reduces the net electrical output available to the served load without directly contributing to electricity delivery. Addressing this engineering problem requires evidence from three interconnected technical domains: variable-speed-drive control of fan and pump auxiliaries, the thermal implications of high-concentration biodiesel blends on engine heat rejection, and the feasibility of renewable-sourced electrical supply for auxiliary loads in isolated-grid environments. Each domain has been investigated independently and, in several cases, within contexts relevant to Indonesian isolated generation. However, the extent to which these bodies of evidence have converged into an integrated auxiliary-load retrofit strategy remains unclear. The following review therefore synthesizes empirical evidence across these three domains, while considering radiator thermal-modelling literature where it informs engineering design and subsequent quantitative validation.

The state of the art across the three constituent domains underpinning this study, namely variable-frequency-drive (VFD) applications for auxiliary and rotating-equipment loads, B40 biodiesel thermal and combustion behavior, and photovoltaic–battery energy storage system (PV–BESS) hybridization for isolated diesel generation, reveals a substantial but fragmented evidence base. Within the Indonesian biodiesel-policy and thermal-performance domain, numerous studies have examined the implementation, operational characteristics, and combustion behavior of high-concentration biodiesel blends, including B40/B50 performance under varying filtration and fuel-temperature conditions and the broader effects of biodiesel fuels on diesel-engine emissions and combustion-chamber behavior [8–19]. Complementary studies addressing feedstock properties and fuel filterability at B30–B40 concentrations further demonstrate that increasing FAME content systematically modifies fuel-handling and combustion characteristics relevant to auxiliary-system design [20, 21]. Nevertheless, none of these studies explicitly quantifies the resulting cooling-system heat-rejection requirements for an isolated diesel generator.

A second, well-established body of literature addresses VFD and variable-speed-drive applications for auxiliary loads. Foundational reviews and case-specific studies covering marine cooling pumps, HVAC chiller fans, induction-motor drives, power-plant boiler air-fan motors, and pump–motor systems consistently report measurable energy savings through speed regulation [22–28]. Closely related research has examined auxiliary and parasitic power optimization in diesel and combined-cycle generation, including genset dispatch optimization in remote diesel–renewable microgrids, variable-speed diesel operation, low-load diesel operation for increased renewable-energy hosting capacity, and reductions in auxiliary consumption through plant-load-factor optimization [29–32]. Collectively, these studies demonstrate that variable-speed auxiliary control is a mature and consistently energy-positive intervention across a wide range of rotating-equipment applications. However, its specific application to radiator cooling fans in isolated PLTDs remains largely undocumented.

A third cluster of literature addresses isolated and off-grid diesel–renewable hybridization relevant to the PLN Nusa Daya operating context. Existing studies encompass photovoltaic–wind–diesel–biomass hybrid systems in the Riau archipelago, biogas- and jatropha-based hybrid generation, techno-economic feasibility assessments for Indonesia's outermost islands, marine-oriented diesel–floating-PV hybrid systems for 3T regions, multi-objective and reliability-oriented hybrid-system sizing, and comparable island-electrification transitions in the Philippines and Pacific region [1–7, 33–40]. Despite their different configurations, these studies generally treat diesel-generator auxiliary consumption, including radiator-fan power, as a fixed operating parameter rather than as a controllable load that could be electrically decoupled and supplied through renewable energy. Broader smart-energy-system literature provides the conceptual basis for treating auxiliary loads as flexible and controllable system elements, a perspective that the present study extends specifically to radiator cooling in isolated PLTDs [41–43].

A systematic literature review previously conducted by the present authors, currently unpublished and performed in accordance with the PRISMA 2020 statement [44], did not identify any published study integrating these three domains into a single retrofit architecture for isolated diesel power plants. More importantly, the review found no study documenting a formal and traceable engineering design process for deriving such a system. Existing auxiliary-load conversion studies typically report the implemented configuration without documenting requirement elicitation, alternative-concept generation, or structured concept selection. Consequently, readers cannot independently evaluate the rationale for selecting a particular configuration over technically plausible alternatives. This absence of design traceability constitutes a methodological gap that is distinct from, and precedes, the quantitative performance gap identified in the systematic review.

This study addresses that methodological gap by presenting, for the first time in the context of isolated diesel power-plant auxiliary systems, the application of a systematic engineering design methodology comprising functional decomposition, morphological analysis, and Pugh-based concept selection, following the VDI 2221/2223 and Pahl & Beitz design frameworks [45–48]. This process derives a modular Renewable-Powered Auxiliary Decoupling (RE-PAD) system for the radiator cooling fan of a B40-fuelled isolated diesel generator. The study aims to systematically elicit functional requirements, generate and evaluate technically feasible alternatives, and establish a traceable modular architecture for decoupling parasitic auxiliary loads in isolated diesel power plants. The resulting architecture provides the conceptual and methodological foundation for subsequent quantitative thermodynamic and techno-economic validation in a companion simulation study currently in preparation.

2. Materials and Methods

2.1. Design Methodology Framework

This study adopts the systematic engineering design methodology established by Pahl and Beitz and formalized in VDI 2221/2223 (Systematic Approach to the Design of Technical Systems) to structure the conceptual development of the Renewable-Powered Auxiliary Decoupling (RE-PAD) system, consistent with recent applications of the VDI 2221 framework in mechanical and product engineering [45–49]. The methodology comprises four sequential phases: task clarification, conceptual design, embodiment design, and detail design. This study is limited to the first two phases, task clarification and conceptual design, and culminates in selecting and specifying a modular system architecture. Embodiment design, detail design, and quantitative thermodynamic and techno-economic validation are reserved for a companion simulation study currently in preparation.

The design process centers on a Caterpillar 3512B LY800217 diesel generator rated at 1024 kW and 1500 rpm, operated under the PLN Nusa Daya Asset Management Contract in Kepulauan Riau, Indonesia. The unit was selected as representative of the 800–1000 kW class of isolated diesel generators that constitutes a substantial proportion of the approximately 80-unit PLN Nusa Daya fleet operating across Riau and Kepulauan Riau provinces.

2.2. Requirement Elicitation

Functional requirements were elicited from four categories of evidence to ensure that the resulting requirement set reflects verifiable engineering, regulatory, and operational conditions rather than unsupported assumptions.

First, direct field measurements were obtained from the demonstration unit, including the crankshaft-to-fan pulley diameters of Ø280 mm and Ø330 mm. These measurements were used to determine the existing fan rotational speed. Because the pulley ratio establishes rotational speed rather than transmitted power, the associated parasitic mechanical load was estimated separately using standard mechanical power relationships.

Second, the current Indonesian biodiesel regulatory framework, particularly Peraturan Menteri ESDM No. 12 Tahun 2023 mandating B40 blending, was reviewed to identify potential implications of the national fuel policy for diesel-engine thermal behavior and cooling-system requirements.

Third, the study incorporated operational constraints specific to the PLN Nusa Daya Asset Management Contract, based on direct managerial experience with the isolated PLTD fleet. These constraints include limitations on modification of primary generating assets and reliability requirements associated with continuous and minimally attended operation. To reduce reliance on managerial recollection alone, the authors cross-checked the experience-based constraints against documented sources, including the scope-of-work provisions of the PLN Nusa Daya Asset Management Contract and applicable operating and maintenance procedures for the isolated PLTD fleet. These documents are retained by the authors and may be made available to the Editors on reasonable request.

Fourth, the authors translated evidence gaps identified through their prior systematic literature review into requirements related to system integration and scalability. The review, currently unpublished, was conducted and reported in accordance with the PRISMA 2020 statement [44]. We retrieved records from five bibliographic databases using search strings combining terms related to variable-frequency drives, biodiesel/B40, parasitic loads, and isolated diesel generation. Inclusion was restricted to peer-reviewed studies published from 2020 onward that addressed at least one of the three constituent domains within stationary or isolated-generation contexts. No published study met the integrated criteria of variable-speed auxiliary control, high-concentration biodiesel operation, and renewable-powered auxiliary decoupling for isolated diesel generation.

2.3. Functional Decomposition

The overall system function was decomposed into sub-functions using a black-box-to-function-tree approach. The system was initially represented as a single transformation of energy, material, and signal inputs into corresponding outputs, then decomposed into a structured chain of sub-functions organized by flow type, following the function-structure convention established by Pahl and Beitz [45, 46].

Sub-function boundaries were defined to correspond to physically or logically separable engineering tasks, including power generation, speed modulation, thermal sensing, control decision-making, and system monitoring. This arrangement allows independent technical alternatives to be assigned to each sub-function during morphological analysis while minimizing ambiguity arising from cross-dependencies.

2.4. Morphological Analysis

Technical alternatives for each sub-function were generated using Zwicky's morphological analysis, which identified two to three candidate solution principles for each sub-function to construct a morphological chart [48]. Candidate alternatives were derived from two principal sources: the literature synthesized in the prior systematic review, particularly studies addressing variable-frequency-drive control, photovoltaic–battery architectures, and thermal-sensing strategies; and benchmarking of components and control practices already established within the PLN Nusa Daya isolated PLTD fleet. This combined approach was adopted to ensure that the generated alternatives remained technically credible and practically deployable under remote operating conditions.

The candidate space was bounded by the functional requirements established during requirement elicitation. Alternatives requiring modification of the engine block or crankshaft were therefore excluded because they conflict with the non-intrusive retrofit requirement (FR3). Likewise, highly automated control configurations inconsistent with the field-maintainability requirement (FR5) were excluded from the principal candidate set.

The adequacy of the alternative space was assessed using three criteria: coverage of the principal solution approaches documented in the literature for each sub-function, commercial availability of the relevant component class in the Indonesian market, and evidence of operational precedent within the PLN Nusa Daya fleet.

Several technically plausible alternatives, including permanent-magnet and brushless-DC motors, centralized energy storage shared across multiple auxiliaries, and predictive or model-based control strategies, were deliberately excluded from the candidate set. This boundary is recognized as a limitation of the conceptual design space and provides a basis for future extension of the RE-PAD architecture.

2.5. Concept Variant Generation

Coherent concept variants were assembled from the morphological chart through compatibility screening rather than exhaustive enumeration of all possible combinations. We evaluated candidate combinations for internal technical consistency and compliance with mandatory functional requirements before formal comparison.

Any combination that retained mechanical coupling between the radiator fan and engine crankshaft while simultaneously claiming elimination of the associated parasitic mechanical load was excluded at this stage. This screening resulted in four internally consistent concept variants: a conventional baseline configuration used as the reference and three progressively decoupled alternatives differentiated primarily by their electrical supply architecture, namely generator-bus-powered, renewable hybrid with fallback supply, and fully dedicated renewable supply, as well as by their control architecture, comprising industrial PLC- and microcontroller-based implementations.

The mandatory screening criterion applied during concept generation concerns only mechanical decoupling from the crankshaft. Electrical decoupling from the generator bus was intentionally retained as a design variable, allowing structured concept selection to determine the relative merits of the alternative electrical supply architectures rather than eliminating them a priori.

2.6. Concept Selection

The four concept variants were evaluated using a Pugh concept selection matrix. The Pugh method was selected instead of a fully quantitative weighted-scoring approach because the conceptual design stage does not provide sufficient numerical evidence to justify precise quantitative weighting. Its ordinal comparison framework, based on whether a concept is better than, equivalent to, or worse than a fixed datum, is also well suited to evaluation by a small expert design-review panel rather than a large stakeholder survey.

The conventional engine-driven configuration (Concept A) was adopted as the fixed datum, consistent with standard Pugh matrix practice. Eight evaluation criteria were applied. Six were derived directly from the functional requirements (FR1–FR6). At the same time, two supplementary criteria, retrofit capital cost and literature-based energy-saving potential, were introduced to incorporate practical and economic considerations that would otherwise be absent from a purely functional comparison.

The criteria were not differentially weighted; each was initially treated as equally important. The author team and the graduate supervisor established scoring by consensus, acting as an informal engineering design-review panel rather than through a numerical stakeholder survey. Pugh's ordinal approach has similarly been employed in small-team product-development applications. At the same time, Quality Function Deployment (QFD) provides an alternative systematic framework that requires explicit quantitative weighting of engineering criteria [50, 51].

The concept achieving the highest net score, calculated as the number of positive assessments minus the number of negative assessments relative to the datum, was selected as the basis for the final architecture.

Because the primary design objective (FR1) influences both the mechanical screening of candidate configurations and the subsequent evaluation of electrical-supply alternatives, we explicitly considered potential circularity. We therefore performed a post-hoc weighting sensitivity analysis to examine whether the ranking remained stable when the equal-weighting assumption was altered. Only final consensus scores were recorded during the panel review; individual pre-consensus scores were not documented, which is acknowledged as a methodological limitation.

2.7. Design Traceability Approach

Following concept selection, a requirement traceability matrix was constructed to determine whether the selected concept, once decomposed into its constituent modules (M1–M6), addresses every functional requirement through at least one identifiable design mechanism.

Each functional requirement was mapped to the module or combination of modules responsible for satisfying it, with a verification statement describing the intended compliance mechanism. This approach follows established systems-engineering practice in which design outputs are systematically mapped against design inputs to identify unaddressed requirements or, conversely, design features lacking explicit functional justification. Comparable requirement-based verification approaches have been reported in other systems-engineering domains [52].

The traceability matrix is intended as a design-consistency assessment rather than quantitative engineering verification or validation. It demonstrates that each functional requirement is addressed by an identifiable design mechanism but does not establish that the mechanism will achieve the required performance under actual operating conditions. Quantitative verification is therefore reserved for subsequent thermodynamic and techno-economic modelling and planned field validation.

2.8. Preliminary Feasibility Screening Approach

A screening-level feasibility assessment was conducted to establish the initial technical plausibility of the selected architecture prior to full quantitative validation. The assessment was deliberately limited in scope and does not constitute a numerical thermodynamic simulation or complete techno-economic analysis.

The screening consisted of two principal components. First, we estimated the magnitude of the parasitic mechanical load potentially eliminated through radiator-fan decoupling algebraically, using the measured belt-drive geometry and standard mechanical power relationships. The resulting value therefore represents an engineering estimate rather than a direct measurement of transmitted shaft power.

Second, the plausible range of fan energy savings was established by comparison with variable-frequency-drive retrofit studies identified in the systematic literature review, including Indonesian and international power-plant auxiliary applications. The potential magnitude of additional cooling demand associated with B40 operation was similarly bounded using previously reported biodiesel combustion and heat-rejection studies.

For this screening, comparator studies were considered sufficiently relevant when three conditions were satisfied: the driven equipment was a fan or pump governed approximately by the affinity-law relationship between rotational speed and power; the motor rating was within the tens-of-kilowatts range relevant to the proposed application; and the operating environment represented a stationary power-plant or industrial auxiliary system rather than a vehicle-traction or laboratory-only application.

This approach is intended solely to establish order-of-magnitude plausibility and should not be interpreted as thermal, operational, or economic validation. Three quantitative parameters associated with the selected architecture are therefore explicitly treated as preliminary. First, the estimated eliminated parasitic load is derived analytically rather than from direct shaft-power measurement. Second, the 43 Hz VFD frequency ceiling is derived from the measured pulley ratio and the specified motor characteristics using the corresponding speed–frequency relationship. Third, the proposed motor/VFD, photovoltaic, and battery capacities represent preliminary design values selected with engineering margin above the estimated peak fan demand.

Formal component sizing requires load-duration analysis, site-specific solar-resource assessment, battery-autonomy and minimum state-of-charge constraints, inverter and conversion efficiencies, and dynamic thermal-load evaluation. These aspects are addressed through the companion quantitative study and may therefore require revising the preliminary component ratings established during the conceptual design stage.

3. Results and Discussion

3.1. Functional Requirements

Six functional requirements formed the basis of the conceptual design process, with each requirement traced to engineering evidence, regulatory conditions, operational constraints, or identified research gaps rather than introduced solely by assumption. Table 1 summarizes these requirements and their corresponding justification sources.

FR1 addresses elimination of the radiator fan's parasitic mechanical load during normal operation. Direct measurement of the crankshaft-to-fan pulley diameters on the Caterpillar 3512B LY800217 (Ø280/Ø330 mm) establishes the existing fan operating speed. At the same time, the associated mechanical power extraction is treated separately as a preliminary engineering estimate. FR2 addresses the cooling system's ability to respond to altered thermal conditions potentially associated with mandatory B40 operation under Peraturan Menteri ESDM No. 12 Tahun 2023, rather than relying on the existing fixed-speed fan configuration.

FR3 and FR4 reflect operational constraints associated with the PLN Nusa Daya Asset Management Contract. Any retrofit intervention must preserve the integrity of the primary generating assets and provide a fail-safe supply path so that failure of the renewable auxiliary system cannot compromise engine cooling or continuity of power generation. FR5 and FR6 extend the requirement set beyond the demonstration unit by recognizing the practical conditions of a geographically dispersed isolated PLTD fleet maintained by field technicians and the need for an architecture that is both maintainable under remote operating conditions and adaptable to other generator units within the target capacity class. Collectively, the requirements presented define the design envelope for functional decomposition, alternative generation, concept selection, and final architecture development.

3.2. Function Structure / Functional Decomposition

Using the black-box-to-function-tree approach, the overall system function was defined as eliminating

Table 1. Functional requirements for the RE-PAD conceptual design, derived from field measurement, regulatory context, operational constraints, and evidence gaps identified in the systematic literature review.

No.	Requirement	Description	Source / Justification
FR1	Parasitic load elimination	The fan drive must be decoupled from the engine crankshaft such that fan operation imposes zero mechanical draw on the generator output circuit.	Field-measured crankshaft-to-fan pulley ratio (Ø280/Ø330 mm), establishing the fan operating speed; the associated continuous mechanical extraction is estimated at 41.0 kW (4.0% of rated output; derivation status in Section 3.8), adopted as a screening estimate within the 3–7% of rated power reported for engine-driven cooling fans.
FR2	B40 compatibility	The system must accommodate the elevated heat rejection requirement associated with B40 biodiesel operation without derating engine output.	Peraturan Menteri ESDM No. 12 Tahun 2023 (mandatory B40 blending); evidence gap RQ2 identified in the prior SLR (zero studies quantify B40 cooling load increment in isolated PLTD context).
FR3	No modification to primary engine/generator systems	Intervention must be limited to the auxiliary cooling circuit; the engine block, generator, and primary electrical distribution must remain unmodified.	Operational constraint under the PLN Nusa Daya Asset Management Contract, where primary generation assets are outside the scope of auxiliary-system retrofit authority.
FR4	Emergency fallback capability	The system must provide a manual bypass path enabling fan operation directly from the AC generator bus in the event of VFD, PV, or BESS failure.	Reliability requirement for isolated PLTD operation, where auxiliary system failure cannot be permitted to compromise continuous power supply.
FR5	Field maintainability by non-specialist technicians	Control logic, components, and diagnostic interfaces must be operable and maintainable by existing PLN field technicians without specialist retraining.	Operational experience within the PLN Nusa Daya isolated PLTD fleet (80 units, Riau and Kepulauan Riau), where specialist technical support is not permanently on-site.
FR6	Fleet scalability	The design must be modular and adaptable to the broader 800–1000 kW class of isolated diesel generators, not limited to the single demonstration unit.	Evidence gap RQ4 identified in the prior SLR (absence of an integrated engineering system applicable across the isolated PLTD fleet).

radiator-fan parasitic load from normal generator operation while maintaining adequate engine thermal management under B40-fuelled operation. Table 2 presents the resulting decomposition into six sub-functions and identifies the associated flow type, inputs, outputs, and functional requirements.

At the black-box level, the system receives engine thermal demand, coolant flow, solar and electrical energy, and temperature information as inputs and produces controlled radiator airflow and regulated coolant temperature as its principal functional outputs. During normal operation, fan power is supplied independently of both the engine crankshaft and generator AC bus. The existing generator bus is retained only as an emergency fallback, consistent with the reliability requirement.

As summarized in Table 2, the energy-flow chain comprising SF1 to SF3 defines how fan rotation is produced, how rotational speed is modulated, and how the required electrical power is supplied independently of the engine shaft during normal operation. These functions primarily address FR1 while providing the controllability required by FR2. The signal-flow chain comprising SF4 and SF5 determines how coolant temperature is sensed and converted into an appropriate fan-speed command, thereby enabling the cooling system to respond to changing thermal demand while remaining transparent and adjustable for field personnel. SF6 provides monitoring and operational logging rather than direct physical control, supporting maintainability, fault identification, and future fleet deployment. The functional structure presented therefore provides the basis for systematically generating technical alternatives.

3.3. Morphological Chart

Table 3 presents the morphological chart developed for the six identified sub-functions, with two to three technically feasible alternatives assigned to each function. These alternatives were derived from solution principles reported in the literature on VFD control, PV-BESS architectures, thermal sensing, and auxiliary-system management, together with components and operating practices considered compatible with the PLN Nusa Daya isolated-PLTD environment. The established functional requirements intentionally bounded the

Table 2. Functional decomposition of the RE-PAD system, presenting its sub-functions, flow types, inputs, outputs, and associated functional requirements.

No.	Sub-function	Flow type	Input	Output	Related FR
SF1	Generate mechanical rotation for fan	Energy	Electrical power (DC/AC)	Fan shaft rotation	FR1
SF2	Modulate fan rotational speed	Energy / Signal	Fixed-speed rotation, control signal	Variable-speed rotation matched to thermal demand	FR1, FR2
SF3	Supply dedicated electrical power to fan drive	Energy	Solar irradiance, stored energy	Regulated DC/AC power to motor	FR1
SF4	Sense coolant thermal state	Signal	Coolant temperature, ambient temperature	Digital/analogue temperature signal	FR2, FR4
SF5	Determine and issue speed command	Signal	Temperature signal, threshold logic	Frequency command to drive	FR2, FR4, FR5
SF6	Display and log system status	Signal	Sensor and control data	Local display, remote monitoring data	FR4, FR5, FR6

Table 3. Morphological chart of the RE-PAD system, presenting the technical alternatives generated for each identified sub-function.

Sub-function	Alternative 1	Alternative 2	Alternative 3
SF1, Generate mechanical rotation	Retain belt-driven mechanical coupling to crankshaft	Electric motor, direct flange-coupled to fan (no gearbox)	Electric motor with gearbox reduction
SF2, Modulate fan speed	Fixed speed (no modulation)	Continuous PID-based speed control	Discrete threshold-based speed control (multi-level)
SF3, Supply power to fan drive	Draw from generator AC bus (existing configuration)	Dedicated PV–BESS supply	Hybrid: PV–BESS primary, AC bus fallback
SF4, Sense coolant thermal state	Single-point analogue sensor (bimetallic)	Dual RTD/thermocouple digital sensing with redundancy	Networked sensor array with SCADA integration
SF5, Determine/issue speed command	Manual technician adjustment	Programmable Logic Controller (PLC), industrial-grade	Microcontroller-based rule logic (e.g., Arduino)
SF6, Display and log system status	No monitoring (as-is)	Local HMI display only	Local HMI + remote logging via Modbus RTU

design space. Alternatives requiring structural modification of the engine block or crankshaft were excluded because they conflict with the non-intrusive retrofit requirement. In contrast, control strategies requiring specialist diagnostic capability or extensive retraining were not prioritized because they conflict with the field-maintainability objective. The resulting alternatives therefore represent a structured design space rather than an exhaustive catalogue of all technically possible solutions, ranging from the existing belt-driven and fixed-speed arrangement to electric fan drives, variable-speed control, renewable-energy supply, redundant sensing, microcontroller control, and remote monitoring. These alternatives were subsequently combined into coherent concept variants.

3.4. Concept Variant Generation

Table 4 presents the four concept variants assembled from the morphological chart and identifies the alternative selected for each sub-function. Compatibility screening was applied before formal comparison to exclude combinations that violated mandatory requirements, particularly those requiring intrusive engine modification. Concept A represents the conventional engine-driven configuration and serves as the reference datum. Concept B replaces the mechanical fan drive with an electrically driven arrangement supplied from the generator bus and controlled through an industrial PLC. Concept C introduces renewable generation and storage while retaining the generator AC bus as part of its hybrid supply architecture. Concept D provides the highest degree of decoupling by combining an electrically driven variable-speed fan with a dedicated renewable-energy and battery supply during normal operation, while retaining the generator bus only as an emergency fallback. Concept D was therefore designated as the proposed RE-PAD architecture.

3.5. Concept Selection Matrix

The four concepts were evaluated using a Pugh selection matrix, with Concept A adopted as the fixed datum. Table 5 compares the concepts across eight criteria: six derived directly from the functional requirements and two supplementary criteria representing retrofit capital cost and literature-based energy-saving potential. Concept B achieved a neutral overall score. Although electrification enables variable-speed control and removes direct mechanical coupling between the crankshaft and fan, the fan remains dependent on generator output for its electrical supply. Consequently, the configuration does not fully achieve normal-operation auxiliary decoupling and is additionally penalized for retrofit cost and field-

Table 4. Concept variants assembled from the morphological chart, showing the combination of alternatives selected per sub-function.

Sub-function	Concept A (Datum)	Concept B	Concept C	Concept D (RE-PAD)
SF1, Fan drive	Belt-driven (Alt.1)	Electric motor, direct-coupled (Alt.2)	Electric motor, direct-coupled (Alt.2)	Electric motor, direct-coupled (Alt.2)
SF2, Speed modulation	Fixed speed (Alt.1)	Continuous PID (Alt.2)	Threshold-based, multi-level (Alt.3)	Threshold-based, multi-level (Alt.3)
SF3, Power supply	AC bus (Alt.1)	AC bus (Alt.1)	Hybrid: PV–BESS + AC fallback (Alt.3)	Dedicated PV–BESS (Alt.2)
SF4, Thermal sensing	Single-point analogue (Alt.1)	Dual RTD/thermocouple (Alt.2)	Dual RTD/thermocouple (Alt.2)	Dual RTD/thermocouple (Alt.2)
SF5, Control logic	Manual adjustment (Alt.1)	PLC, industrial-grade (Alt.2)	Microcontroller-based (Alt.3)	Microcontroller-based (Alt.3)
SF6, Monitoring	No monitoring (Alt.1)	Local HMI only (Alt.2)	Local HMI + Modbus RTU (Alt.3)	Local HMI + Modbus RTU (Alt.3)

Table 5. Pugh concept selection matrix, evaluating alternative concepts against criteria derived from the functional requirements. Concept A (conventional system) serves as the datum. Scoring: + (better than datum), S (same as datum), − (worse than datum).

Criterion (source FR)	Concept A (Datum)	Concept B	Concept C	Concept D (RE-PAD)
Parasitic load elimination (FR1)	S	S	S	+
B40 thermal adequacy (FR2)	S	+	+	+
No engine/generator modification (FR3)	S	S	S	S
Emergency fallback reliability (FR4)	S	S	+	+
Field maintainability, non-specialist (FR5)	S	−	+	+
Fleet scalability (FR6)	S	S	+	+
Retrofit capital cost	S	−	−	−
Energy saving potential (literature-based)	S	+	S	+
Sum (+)	0	2	4	6
Sum (−)	0	2	1	1
Net score	0	0	3	5

maintainability requirements associated with industrial PLC control. Concept C achieved a net score of +3 because its hybrid renewable architecture improves thermal control, reliability, maintainability, and scalability. However, the generator AC bus remains part of its routine supply architecture, meaning it does not achieve complete electrical independence from the generator. Concept D achieved the highest net score of +5, primarily because it combines complete mechanical decoupling with normal-operation electrical independence through a dedicated PV-BESS supply. However, this advantage comes with a higher initial investment. The preference for Concept D therefore reflects stronger satisfaction of the primary decoupling objective rather than an assumed thermal-performance advantage.

Because Concepts C and D initially received the same capital-cost penalty despite their different investment requirements, Table 6 presents a sensitivity analysis using a refined cost penalty and alternative weighting scenarios. Under equal weighting with refined cost scoring, Concept D remains preferred with a score of +4 compared with +3 for Concept C, and it also remains preferred when FR1 receives double weighting. The two concepts become equivalent when capital cost is weighted twice as strongly, whereas Concept C becomes preferred when capital cost receives triple weighting. These results show that Concept D selection depends on the relative priority assigned to auxiliary-load decoupling and capital expenditure, and that sites under strong investment constraints may rationally prefer Concept C despite its lower degree of electrical decoupling.

3.6. Final RE-PAD Architecture

Concept D was subsequently developed into a modular architecture comprising six functionally distinct but operationally integrated modules, M1 to M6. Figure 1 illustrates the overall RE-PAD configuration and its energy, coolant, sensing, and control pathways, while Table 7 summarizes the principal components and design rationale associated with each module.

The original mechanical coupling between the engine crankshaft and radiator fan is replaced by a directly coupled electric motor controlled through a variable-frequency drive. Based on the measured crankshaft and fan pulley diameters of 280 mm and 330 mm, respectively, the original radiator fan operates at approximately 1272.7 rpm when the engine runs at its rated speed of 1500 rpm. The replacement system uses a four-pole induction motor with a synchronous speed of 1500 rpm at 50 Hz. To reproduce the original fan rotational speed, the corresponding VFD frequency is approximately 42.4 Hz. Therefore, a maximum normal operating frequency of 43 Hz is specified. Considering normal induction-motor slip under load, this setting maintains the fan speed close to its original operating

Table 6. Weighting sensitivity check on the Pugh ranking. Cost scoring refined to −1 (Concept C) and −2 (Concept D).

Scenario	Concept B	Concept C	Concept D	Preferred
Equal weighting, refined cost	0	3	4	D
FR1 double-weighted	0	3	5	D
Capital cost double-weighted	−1	2	2	C ≈ D (tie)
Capital cost triple-weighted	−2	1	0	C

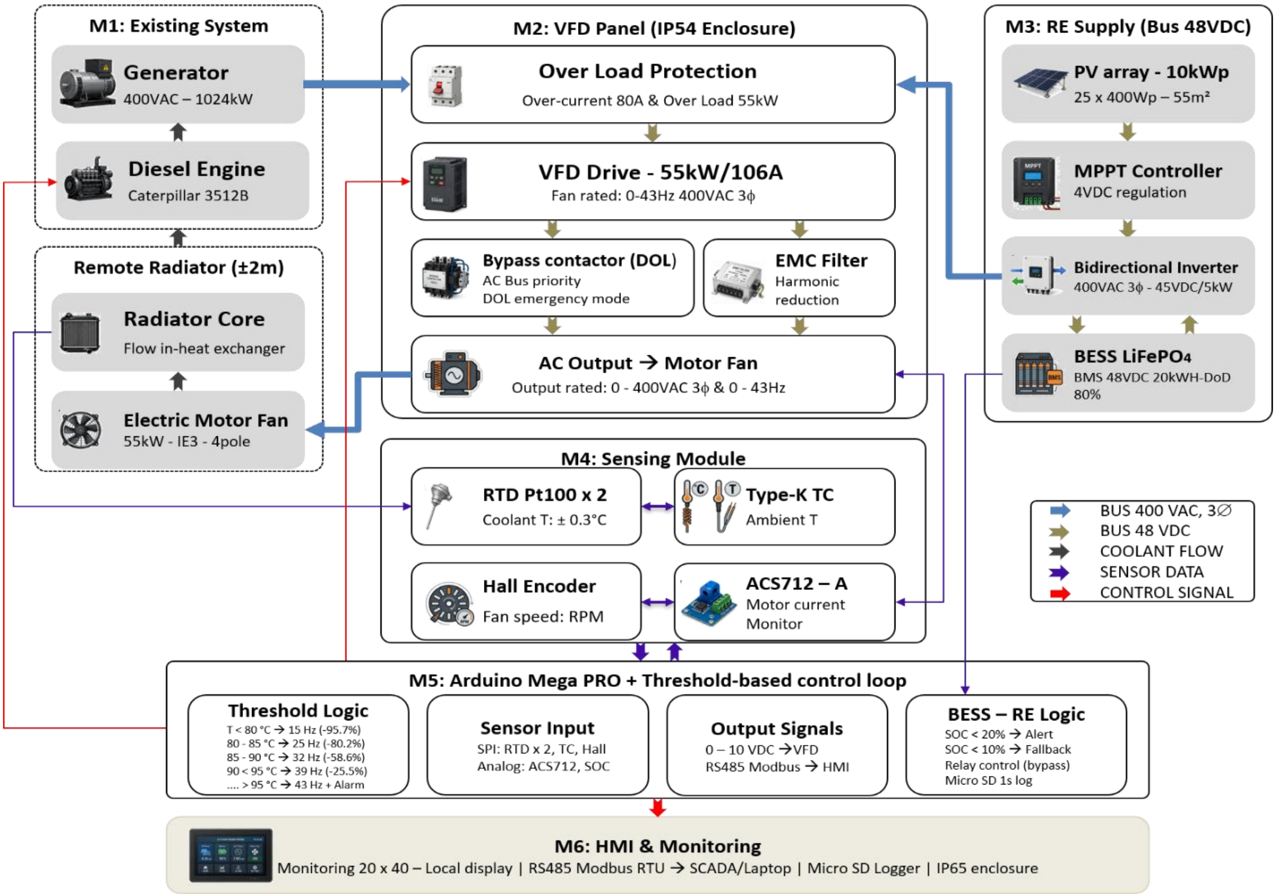

Figure 1. RE-PAD modular retrofit architecture (M1–M6) for the Caterpillar 3512B LY800217, 1024 kW, Kepulauan Riau. Arrows denote AC power (blue), 48V RE/DC supply (amber), coolant flow (grey), sensor data (purple), and control signal (red).

Table 7. RE-PAD module specifications, key components, and design rationale, traced to sub-functions.

No.	Module	Key components	Related SF	Design rationale
M1	Mechanical interface	Universal adapter bracket; axial fan Ø1000 mm; direct flange coupling (no belt)	SF1	Preserves existing radiator housing; belt-pulley system removed entirely; no engine block modification required
M2	Power & protection	MCB 80A; MCCB 80A; VFD (55 kW/106 A); bypass contactor; EMC filter	SF1, SF2	Maximum output frequency locked at 43 Hz to prevent fan overspeed (belt ratio 280/330 = 0.8485); bypass enables direct-online emergency operation from AC bus without VFD
M3	RE supply	PV 10 kWp; MPPT 60A/48V; BESS LiFePO4 20 kWh 48V; bidirectional inverter	SF3	Fan motor fully powered by dedicated RE supply; zero parasitic draw on generator; AC genset bus serves as automatic fallback when BESS state of charge falls below threshold
M4	Sensing	Dual RTD Pt100; Type-K thermocouple; Hall encoder; current sensor; BESS SOC monitor	SF4	Redundant sensing streams provide fault-tolerant thermal data for the control logic
M5	Control & logic	Microcontroller (Arduino Mega PRO); DAC; RS485 transceiver; relay modules	SF5	Rule-based, five-level threshold logic selected over PID for robustness under industrial noise and ease of field tuning by non-specialist PLN technicians
M6	HMI & monitoring	Local LCD display; RS485 Modbus RTU; data logger; industrial enclosure	SF6	Provides real-time visibility and historical logging for maintenance verification and future SCADA integration

Table 8. Requirement traceability matrix, tracing each functional requirement to the module or modules of the selected RE-PAD architecture.

Requirement	Addressed by module(s)	Traceability statement
FR1: Parasitic load elimination	M1, M2, M3	Mechanical decoupling (M1) combined with dedicated RE supply (M3) removes the fan entirely from the generator power circuit; VFD frequency ceiling (M2) prevents any reintroduction of mechanical overspeed risk.
FR2: B40 compatibility	M2, M4, M5	Variable-speed control responsive to real-time coolant sensing (M4) provides the mechanism by which the elevated heat rejection associated with B40 can be accommodated without a fixed-speed constraint; whether the selected fan, motor, and radiator jointly deliver the required heat-rejection capacity under B40 conditions is a performance question addressed by the ε-NTU thermal model in the companion study, not established by this mapping.
FR3: No engine/generator modification	M1	Intervention is confined to the fan drive and radiator relocation; no modification to the engine block, crankshaft, or generator is required
FR4: Emergency fallback	M2, M3	Safe bypass behaviour during VFD, PV, or BESS failure is a performance property to be confirmed in the companion study and field campaign.
FR5: Field maintainability	M5, M6	Microcontroller-based rule logic (M5) and local HMI (M6) are field-adjustable without specialist retraining, in contrast to PLC-based alternatives screened out in Section 3.5.
FR6: Fleet scalability	M1–M6 (modular)	Independently replaceable module boundaries allow component re-sizing for the broader 800–1000 kW generator class without redesigning the overall architecture.

value while reducing the risk of overspeed during normal VFD-controlled operation.

The VFD and protection hardware are incorporated within M2, while the dedicated renewable supply is provided through M3 using a preliminary 10 kWp photovoltaic array and 20 kWh LiFePO4 battery system. The generator AC bus remains available only as an emergency supply path when predetermined fallback conditions occur. During normal operation, FR1 is therefore achieved through two complementary mechanisms: removal of mechanical power extraction from the crankshaft and electrical independence from the generator bus. The architecture is not unconditionally isolated from the generator because the AC bus remains available during low battery state of charge or failure of the renewable supply path.

Dual temperature sensing provides redundant thermal-state information, while a five-level threshold controller determines the required fan speed. This redundant sensing arrangement follows established practice in shell-and-tube and multi-channel heat-exchanger instrumentation, where accurate thermal-coefficient determination depends on redundant temperature sensing under variable flow conditions [53].

Threshold-based control was selected over a more complex continuous-control strategy because it provides transparent field adjustment and simpler fault diagnosis under remote operating conditions. The normal energy pathway proceeds from the renewable-supply module through the power-conversion and motor-drive system to the radiator fan, while the generator AC bus remains physically available as a separate emergency pathway.

The preliminary component ratings, including the 55 kW/106 A VFD, 10 kWp photovoltaic array, and 20 kWh battery storage, should be interpreted as conceptual placement values rather than final sizing results. Final sizing requires site-specific load-duration analysis, solar-resource characterization, battery-autonomy limits, conversion losses, seasonal variability, and fallback frequency.

3.7. Requirement Traceability Matrix

Table 8 presents the requirement traceability matrix linking each functional requirement to the module or combination of modules responsible for addressing it. The matrix indicates that all six elicited requirements have at least one corresponding architectural response and that each principal module has an explicit functional purpose. FR1 is addressed through the combined action of the mechanical interface, VFD drive, and dedicated renewable supply, while FR2 is addressed through variable-speed control, temperature sensing, and control logic. FR4 is supported through the retained emergency supply path, whereas FR5 is addressed through field-adjustable microcontroller logic and local monitoring. The modular architecture supports FR6 by allowing major components to be resized without altering the underlying system structure. This mapping demonstrates internal design consistency but should not be interpreted as quantitative engineering verification, since thermal adequacy, renewable-energy availability, fail-safe reliability, and component performance still require numerical and experimental confirmation.

3.8. Preliminary Feasibility Screening

A preliminary feasibility assessment used order-of-magnitude engineering estimates and evidence from analogous applications rather than numerical simulation. The parasitic mechanical load associated with the existing radiator fan was provisionally represented as approximately 4.0% of rated generator output, corresponding to approximately 41.0 kW for the 1024 kW Caterpillar 3512B LY800217.

This value should not be interpreted as a direct result of the pulley measurement. The measured pulley ratio establishes fan rotational speed only, while the 4.0% value represents a screening estimate selected within the broader range reported for mechanically driven cooling fans in comparable applications. Direct measurement of fan power is therefore required before the 41.0 kW value can be considered unit-specific empirical evidence.

Comparable VFD studies reported energy reductions of approximately 30 to 60% across stationary fan and pump applications [22–28], including approximately 32% annual savings for a boiler air-fan retrofit in an Indonesian steam power plant [27]. These values support the technical plausibility of variable-speed fan operation but should not be interpreted as predicted savings for the RE-PAD configuration.

Similarly, the cited biodiesel literature indicates that high-concentration biodiesel can alter combustion and thermal behavior [10, 18, 19]. However, the specific magnitude of additional radiator heat-rejection demand for the Caterpillar 3512B under B40 operation remains unquantified. Consequently, the 41.0 kW parasitic-load estimate, VFD saving range, and potential B40 thermal influence should all be treated as screening parameters pending quantitative modelling and field measurement.

3.9. Interpretation of the Design Process and Selected Architecture

The combined use of functional decomposition, morphological analysis, compatibility screening, and Pugh-based selection provides a traceable explanation for why the RE-PAD architecture emerged from the conceptual design process.

The difference between Concept D (+5) and Concept C (+3) is not evidence of superior thermal performance. Rather, it reflects the greater extent to which Concept D satisfies the principal functional requirement for normal-operation auxiliary decoupling and its stronger assessed energy-saving potential.

The sensitivity analysis further demonstrates that this preference is not unconditional. Concept D remains preferred when the main design objective is weighted heavily, but Concept C becomes increasingly competitive as capital cost receives greater weighting. The selection therefore represents an explicit engineering trade-off between decoupling performance and investment burden.

The relationship between the selected concept and the original design requirements further confirms that the RE-PAD architecture most completely satisfies the stated requirements within the defined candidate space and evaluation assumptions, rather than being a universally optimal solution.

3.10. Comparison with Prior Engineering and Literature

Within the literature considered in the authors' prior review, no study documents an equivalent requirement-driven design process for converting an isolated diesel-generator radiator fan from mechanical drive to a renewable-powered, variable-speed auxiliary architecture.

Existing VFD studies demonstrate the technical value of speed control for pumps and fans in marine, industrial, and power-generation applications [22–28]. However, the reviewed studies do not address the specific combination of an isolated PLTD radiator fan, B40 fuel operation, dedicated renewable auxiliary supply, and structured engineering concept selection.

Related precedents exist in automotive thermal-management research, where electric variable-speed fans and coolant pumps have been used to reduce auxiliary demand while maintaining temperature control [54]. The contribution of the present study therefore lies primarily in the systematic design methodology and its application context rather than in claiming that electric variable-speed cooling itself is technically unprecedented.

The overall design process provides a traceable chain from requirement definition and functional decomposition through alternative generation, concept selection, architecture development, and requirement mapping. This design traceability distinguishes the present approach from auxiliary retrofit studies that report only the final implemented configuration.

3.11. Practical and Fleet-Scale Implications

The modular M1 to M6 architecture has potential implications for application across the broader PLN Nusa Daya isolated PLTD fleet. Key components such as the electric motor, VFD, photovoltaic array, and BESS can in principle be re-sized without changing the underlying functional architecture.

This modularity could support phased implementation, with candidate units prioritized by generator capacity, fuel-logistics cost, operating profile, renewable-resource availability, or retrofit economics. The retained AC-bus emergency fallback also provides a practical transition mechanism by ensuring that cooling continuity does not initially depend solely on an unproven renewable auxiliary supply.

These implications nevertheless represent conceptual scalability rather than demonstrated fleet-wide applicability. The component specifications were developed around the Caterpillar 3512B reference unit. Differences in radiator geometry, fan diameter, airflow requirements, coolant characteristics, shaft power, operating speed, and electrical configuration across other generator models must therefore be evaluated before transferring the architecture to other units.

3.12. Limitations of the Conceptual Design Approach

Several limitations constrain interpretation of the present design. First, the feasibility assessment is based on engineering screening and analogous literature rather than unit-specific simulation or measured performance. The reported VFD saving ranges, parasitic-load estimate, and potential B40 thermal effects therefore remain preliminary.

Second, the author team and graduate supervisor conducted concept selection rather than a larger independent or multi-stakeholder panel. Although the sensitivity analysis improves transparency regarding weighting assumptions, it does not remove the subjectivity inherent in small-team evaluation. This risk is documented more broadly in studies of expert group decision-making in engineering consulting contexts [55].

Third, several requirements were informed by operating experience within a single PLN Nusa Daya asset-management context and may not fully represent other isolated-generation settings.

Fourth, the morphological design space was deliberately restricted to a limited number of field-realistic alternatives. We did not evaluate other technically plausible options, including permanent-magnet motors, brushless-DC drives, centralized auxiliary storage, predictive control, model-based control, and alternative renewable-supply architectures. Concept D should therefore be interpreted as the preferred configuration within the evaluated design space rather than a global optimum.

Fifth, the authors recorded only final consensus scores during concept evaluation. Individual pre-consensus assessments and independent evaluator scores were not available. Finally, fleet scalability remains conceptual and has not yet been verified through multi-unit sizing analysis.

3.13. Positioning Relative to Quantitative Validation and Future Research

The conceptual architecture developed in this study is intended as a precursor to quantitative engineering validation, not a substitute for it. The proposed component specifications and functional mechanisms require subsequent confirmation through thermal, electrical, economic, and experimental analyses.

Future quantitative work will evaluate radiator thermal behavior using an ε-NTU model combined with fan affinity relationships, photovoltaic generation, battery operation, and auxiliary-load profiles. Techno-economic indicators including payback period, net present value, internal rate of return, and sensitivity to major technical and economic parameters will then determine whether the conceptual advantages identified in this study translate into operational and financial benefits.

A subsequent field campaign on an operational Caterpillar 3512B unit will also measure actual fan demand, coolant and ambient temperatures, fan-speed behavior, renewable-energy contribution, and fallback frequency. Future research may additionally extend the design methodology to other auxiliary loads and incorporate multiple operating sites and independent stakeholders to evaluate the broader generalizability of the RE-PAD concept.

4. Conclusions

This study applied the Pahl and Beitz/VDI 2221–2223 systematic design framework to develop a modular Renewable-Powered Auxiliary Decoupling (RE-PAD) architecture for the radiator cooling fan of a B40-fuelled isolated diesel generator. Requirement elicitation, morphological analysis, and Pugh-based concept selection identified the fully decoupled photovoltaic–battery configuration as the preferred concept. In contrast, requirement traceability confirmed that the selected six-module architecture addressed all defined functional requirements at the conceptual level. Preliminary feasibility screening indicated that the proposed design is technically plausible relative to comparable VFD and biodiesel-related studies; however, the estimated 41.0 kW parasitic load, component ratings, energy-saving potential, and thermal adequacy under B40 operation still require quantitative validation. This study therefore provides a formal, traceable engineering design process for isolated diesel auxiliary retrofits, offering a structured foundation for subsequent thermodynamic, techno-economic, and field validation.

Author Contributions: Conceptualization, M.M. and E.Y.; methodology, M.M.; validation, A.R.W., A.F., and E.Y.; formal analysis, M.M. and R.F.F.; investigation, M.M. and D.P.N.; resources, M.M.; writing—original draft preparation, M.M.; writing—review and editing, E.Y., A.Z.T., and A.S.U.; visualization, M.M.; supervision, E.Y.; project administration, M.M. All authors have read and agreed to the published version of the manuscript.

Funding: This study does not receive external funding.

Ethical Clearance: Not applicable.

Informed Consent Statement: Not applicable.

Data Availability Statement: The data supporting the findings of this study, including field measurement records and design evaluation matrices, are available from the corresponding author upon reasonable request.

Acknowledgments: The authors thank PT PLN Nusa Daya for providing access to operational data and field measurements for the Caterpillar 3512B LY800217 unit, and the Graduate School of Renewable Energy, Darma Persada University, for academic supervision and support.

Conflicts of Interest: All the authors declare no conflicts of interest.

References

1. Baqaruzi, S., Muhtar, A., Prasetyawan, P., Kanata, S., and Winata, T. (2022). Economic-Environmental Study on Hybrid System of Photovoltaic, Wind, Diesel, Biomass for Off-Grid Rural Electrification in Sebesi Island, Indonesia, *International Review of Electrical Engineering (IREE)*, Vol. 17, No. 4, 382. doi:10.15866/iree.v17i4.21002.
2. Castro, M. T., Delina, L. L., and Ocon, J. D. (2024). Transition Pathways to 100 % Renewable Energy in 208 Island Mini-Grids in the Philippines, *Energy Strategy Reviews*, Vol. 52, 101315. doi:10.1016/j.esr.2024.101315.
3. Prasad, S. S., and Singh, A. (2020). Economic Feasibility of Biodiesel Production from Pongamia Oil on the Island of Vanua Levu, *SN Applied Sciences*, Vol. 2, No. 6, 1086. doi:10.1007/s42452-020-2883-0.
4. García-Mariaca, A., Villalba, J., Carreño, U., and Aldana, D. (2023). Performance and Emissions of a CI-ICE Fuelled with Jatropha Biodiesel Blends and Economic and Environment Assessment for Power Generation in Non-Interconnected Areas, *Energies*, Vol. 16, No. 16. doi:10.3390/en16165964.
5. Castro, M. T., Pascasio, J. D. A., and Ocon, J. D. (2022). Data on the Techno-Economic and Financial Analyses of Hybrid Renewable Energy Systems in 634 Philippine off-Grid Islands, *Data in Brief*, Vol. 44, 108485. doi:10.1016/j.dib.2022.108485.
6. Subekti, L., Nugraha, C. F., Arrofiq, M., Muthahhari, A. A., Prasetyo, B. E., and A'yun, Q. (2024). Techno-Economic Analysis for Raja Ampat Off-Grid System, *Jurnal Nasional Teknik Elektro*, Vol. 13, No. 1, 42–50. doi:10.25077/jnte.v13n1.1180.2024.
7. Pribadi, R. A., and Syafii. (2023). Optimal Design and Economic Analysis of Biogas/Diesel/PV Power System for Electrification of Palm Oil Factory and Surround Settlements, *2023 International Conference for Advancement in Technology (ICONAT)*, IEEE, 1–4. doi:10.1109/ICONAT57137.2023.10080365.
8. Farobie, O., and Hartulistiyoso, E. (2021). Palm Oil Biodiesel as a Renewable Energy Resource in Indonesia: Current Status and Challenges, *BioEnergy Research*, Vol. 15, No. 1, 93–111. doi:10.1007/S12155-021-10344-7.
9. Wirawan, S. S., Solikhah, M. D., Setiapraja, H., and Sugiyono, A. (2024). Biodiesel Implementation in Indonesia: Experiences and Future Perspectives, *Renewable and Sustainable Energy Reviews*, Vol. 189, 113911. doi:10.1016/j.rser.2023.113911.
10. Nguyen, V. G., Pham, M. T., Le, N. V. L., Le, H. C., Truong, T. H., and Cao, D. N. (2023). A Comprehensive Review on the Use of Biodiesel for Diesel Engines, *International Journal of Renewable Energy Development*, Vol. 12, No. 4, 720–740. doi:10.14710/ijred.2023.54612.
11. Nagappan, M., Boomadevi, P., Ommurugadhasan, D., Jayaprabakar, J., Durairaj, R. B., and Sudhakar, K. (2026). Alternate Fuels for Internal Combustion Engines: Status Review on Improving Performance and Reducing Emissions with Biodiesel, Bio-alcohol, Bio-oil and Plastic Oil, *Environmental Progress & Sustainable Energy*, 70485. doi:10.1002/ep.70485.
12. Selvam, M., Pragadish, N., Harish, K. A., Srinivasan, R. G., Devarajan, Y., and Kaliappan, N. (2025). Investigating Emission Characteristics and Combustion Performance of a CRDI Engine Utilizing Novel Biodiesel Derived from Waste Cooking Oil and Pentanol Blends, *Scientific Reports*, Vol. 15, No. 1, 14742. doi:10.1038/s41598-025-98462-6.
13. Kandasamy, V. K., Dhairiyasamy, R., and Rajendran, S. (2024). Experimental Investigation of Cottonseed Biodiesel and Biodiesel Blends in a 14 KW Diesel Generator: Effects on Performance, Emissions, and Engine Parameters, *Advanced Engineering Forum*, Vol. 51, 75–91. doi:10.4028/p-S9sRZ1.
14. Wang, Z., Chen, Y., He, C., Wang, D., Nie, Y., and Li, J. (2025). Effect of Improved Combustion Chamber Design and Biodiesel Blending on the Performance and Emissions of a Diesel Engine, *Energies*, Vol. 18, No. 11, 2956. doi:10.3390/EN18112956.
15. Uhanto, U., Yandri, E., Hilmi, E., Saiful, R., and Ariati, R. (2025). Evaluating Engine Durability and Operational Effects of Biodiesel Blends in Heavy Equipment Applications, *Next Energy*, Vol. 9, 100392. doi:10.1016/j.nxener.2025.100392.
16. Purbandono, D. A., Budiyanto, M. A., Ramdan, F., and Felani, M. I. (2025). Optimization of Load Distribution and Fuel Consumption for Diesel Generator 1000 KW for Remote Area Using Biodiesel B35 Power Station, *Eastern-European Journal of Enterprise Technologies*, Vol. 3, No. 8 (135), 42–59. doi:10.15587/1729-4061.2025.327179.
17. Romy, R., Helwani, Z., and Felix Mandrofa, A. (2022). Study Experimental of Diesel Engines Performance by Using Variations of Mesh Filter and Biodiesel B40, B50 as Fuel, *The Journal of Ocean, Mechanical and Aerospace -Science and Engineering- (JOMAse)*, Vol. 66, No. 3, 103–109. doi:10.36842/jomase.v66i3.291.
18. Wisnu, D., and Romy, R. (2023). Study Experimental of Temperature Effect of B40 Biodiesel Engine Performance, *The Journal of Ocean, Mechanical and Aerospace -Science and Engineering- (JOMAse)*, Vol. 67, No. 1, 7–14. doi:10.36842/jomase.v67i1.301.
19. Semin, Cahyono, B., Listyanto, H. A., and Bakar, R. A. (2020). Analysis of the Performance of Diesel Engine Fueled Using B50-B100 Biodiesel Based on Simulation, *International Journal of Marine Engineering Innovation and Research*, Vol. 5, No. 3, 180–189. doi:10.12962/J25481479.V5I3.
20. Boichenko, S., Yakovlieva, A., Zubenko, S., and Shkilniuk, I. (2025). Physical, Chemical, and Performance Properties of Biodiesel Fuels: A Comparative Study of Lipid-Based Feedstocks, *Energies*, Vol. 18, No. 16, 4274. doi:10.3390/en18164274.
21. Pramudito, Y., Fathurrahman, N. A., Auzani, A. S., Wibowo, C. S., Anggarani, R., Soemanto, A., and Sugiarto, B. (2023). Comparative Analysis of Filterability Behavior of B30 and B40 Biodiesel Blends on Various Porosity and Dimension of Fuel

Filter, *International Journal of Renewable Energy Development*, Vol. 12, No. 4, 760–767. doi:10.14710/ijred.2023.52801.

22. Sadek, M., El-Maghraby, R., and Fathy, M. (2023). Evaluation of Variable Speed Drives to Improve Energy Efficiency and Reduce Gas Emissions: Case Study, *Chemical Industry and Chemical Engineering Quarterly*, Vol. 29, No. 2, 111–118. doi:10.2298/CICEQ220318018S.

23. Kapp, S., Wang, C., McNelly, M., Romeiko, X., and Choi, J.-K. (2024). A Comprehensive Analysis of the Energy, Economic, and Environmental Impacts of Industrial Variable Frequency Drives, *Journal of Cleaner Production*, Vol. 434, 140474. doi:10.1016/j.jclepro.2023.140474.

24. Rayhan, F. A., and Alma, R. (2026). Energy Efficiency Analysis of Main Cooling Pump System on Bulk Carrier Using VSD, *Indonesian Journal of Maritime Technology (ISMATECH)*. doi:10.35718/ismatech.v4i1.8481980.

25. Hassan, W., Mahmood, F., Akmal, M., and Nasir, M. (2020). Optimum Operation of Low Voltage Variable-frequency Drives to Improve the Performance of Heating, Ventilation, and Air Conditioning Chiller System, *International Transactions on Electrical Energy Systems*, Vol. 30, No. 9. doi:10.1002/2050-7038.12481.

26. Dinolova, P., Ruseva, V., and Dinolov, O. (2023). Energy Efficiency of Induction Motor Drives: State of the Art, Analysis and Recommendations, *Energies*, Vol. 16, No. 20, 7136. doi:10.3390/en16207136.

27. Wibowo, P. M., Haddin, M., and Marwanto, A. (2021). Energy Saving Analysis of Air Fan Motor in Power Plant Boiler Controlled by Variable Frequency Drive, *International Journal of Power Electronics and Drive Systems (IJPEDS)*, Vol. 12, No. 4, 2059. doi:10.11591/ijpeds.v12.i4.pp2059-2069.

28. Salama, M. A. E., El-Naggar, N. M., and Abu-Zaid, S. (2024). Energy Saving Analysis for Pump-Motor Set in Water Purification Plant Using Variable Speed Drive, *Scientific Reports*, Vol. 14, No. 1, 27728. doi:10.1038/s41598-024-75601-z.

29. Matragi, I., Maiboom, A., Tauzia, X., Moricet, B., and Thevenoux, Y. (2024). A Novel Algorithm for Optimizing Genset Operations to Minimize Fuel Consumption in Remote Diesel-RES Microgrids, *Energy Conversion and Management: X*, Vol. 24, 100728. doi:10.1016/J.ECMX.2024.100728.

30. Wang, H., and Yun, Q. (2023). Research on Speed Optimization and Adjusting Strategy of Variable Speed Diesel Generator Base on Sliding Interval, *Journal of Marine Science and Engineering*, Vol. 11, No. 9, 1682. doi:10.3390/jmse11091682.

31. Hamilton, J., Negnevitsky, M., Wang, X., and Semshchikov, E. (2020). The Role of Low-Load Diesel in Improved Renewable Hosting Capacity within Isolated Power Systems, *Energies*, Vol. 13, No. 16, 4053. doi:10.3390/en13164053.

32. Gavirineni, N. K., and Gundabattini, E. (2022). Enhancing the Energy Efficiency of a Supercritical Thermal Power Plant Through Improved Plant Load Factor, and Optimized Performance of Auxiliary Equipment, *International Journal of Design & Nature and Ecodynamics*, Vol. 17, No. 2, 177–187. doi:10.18280/ijdne.170203.

33. Muhtar, A., Prasetyawan, P., Kanata, S., Baqaruzi, S., and Winata, T. (2021). Economic and Environmental Assessment of the Implementation of Hybrid Auto-Size Diesel Generators with Renewable Energy on Sebesi Island, *2021 3rd International Conference on High Voltage Engineering and Power Systems (ICHVEPS)*, IEEE, 288–293. doi:10.1109/ICHVEPS53178.2021.9601124.

34. Vaka, S. S. K. R., and Matam, S. K. (2023). Optimal Sizing of Hybrid Renewable Energy Systems for Reliability Enhancement and Cost Minimization Using Multiobjective Technique in Microgrids, *Energy Storage*, Vol. 5, No. 4. doi:10.1002/est2.419.

35. Z Day, F. H., Samual, M. G., Garniwa, I., and Sudiarto, B. (2024). Techno-Economic Optimization Study of Renewable Energy Planning in Buru Island Electricity System, *International Journal of Electrical, Computer, and Biomedical Engineering*, Vol. 2, No. 4. doi:10.62146/ijecbe.v2i4.73.

36. Nugraha, C. F., Subekti, L., Muthahhari, A. A., Prasetyo, B. E., and Budi, R. F. S. (2024). A SUSTAINABLE HYBRID OFF-GRID SYSTEM DESIGN FOR ISOLATED ISLAND CONSIDERING TECHNO-ECONOMIC AND FREQUENCY STABILITY ANALYSIS, *Journal of Applied Engineering and Technological Science*, Vol. 6, No. 1, 444–464. doi:10.37385/JAETS.V6I1.4892.

37. Trombley, J. B., Sangha, K. K., Andersen, A. N., and Thennadil, S. N. (2023). Utilizing Locally Available Bioresources for Powering Remote Indigenous Communities: A Framework and Case Study, *Energies*, Vol. 16, No. 2, 666. doi:10.3390/en16020666.

38. Rosyid, O. A., Taradini, A., Hartadhi, Lande, N. M., Andrianshah, Sutrisno, B., Kamil, B., Khairiani, D., Hartadi, T., Sudrajat, A., and Tarno. (2024). Marine-Based Renewable Energy Solution for 3T Areas in Indonesia: Integrating Diesel Hybridization with Floating PV Power Plant, *BIO Web of Conferences*, Vol. 92, 01009. doi:10.1051/bioconf/20249201009.

39. Shafira, A. N., Petrana, S., Muthia, R., and Purwanto, W. W. (2023). Techno-Economic Analysis of a Hybrid Renewable Energy System Integrated with Productive Activities in an Underdeveloped Rural Region of Eastern Indonesia, *Clean Energy*, Vol. 7, No. 6, 1247–1267. doi:10.1093/ce/zkad068.

40. Wijaya, M. H. P., Setyonegoro, M. I. B., and Ali, H. R. (2024). Techno-Economic Feasibility Analysis of a Hybrid Renewable Energy System for Gili Labak Island as a Disadvantaged, Outermost and Frontier Region of Indonesia Using HOMER, *2024 16th International Conference on Information Technology and Electrical Engineering (ICITEE)*, IEEE, 428–433. doi:10.1109/ICITEE62483.2024.10808921.

41. Liu, F., Su, C. W., Qin, M., and Umar, M. (2023). Is Renewable Energy a Path towards Sustainable Development?, *Sustainable Development*, Vol. 31, No. 5, 3869–3880. doi:10.1002/sd.2631.

42. Zhao, N., Zhang, H., Yang, X., Yan, J., and You, F. (2023). Emerging Information and Communication Technologies for Smart Energy Systems and Renewable Transition, *Advances in Applied Energy*, Vol. 9, 100125. doi:10.1016/j.adapen.2023.100125.

43. Kabeyi, M. J. B., and Olanrewaju, O. A. (2023). Smart Grid Technologies and Application in the Sustainable Energy Transition: A Review, *International Journal of Sustainable Energy*, Vol. 42, No. 1, 685–758. doi:10.1080/14786451.2023.2222298.

44. Page, M. J., McKenzie, J. E., Bossuyt, P. M., Boutron, I., Hoffmann, T. C., Mulrow, C. D., Shamseer, L., Tetzlaff, J. M., Akl, E. A., Brennan, S. E., Chou, R., Glanville, J., Grimshaw, J. M., Hróbjartsson, A., Lalu, M. M., Li, T., Loder, E. W., Mayo-Wilson, E., McDonald, S., et al. (2021). The PRISMA 2020 Statement: An Updated Guideline for Reporting Systematic Reviews, *BMJ*, n71. doi:10.1136/bmj.n71.

45. Schilling, L., Spitzer, S., Kupfer, R., Klaus, C., and Gude, M. (2025). Integrating Environmental Assessment into Aerospace Product Development Using the VDI 2221 Methodology, *Discover Sustainability*, Vol. 6, No. 1, 809. doi:10.1007/s43621-025-01762-0.

46. Wijaya, D. K., Hartono, B. J. R., Jazuli, J., and Izzhati, D. N. (2024). Optimizing Product Design and Development of Engine Carbon Cleaning Maintenance Tools Using Reverse Engineering and VDI 2222 Methods, *OPSI*, Vol. 17, No. 1, 185–203. doi:10.31315/OPSI.V17I1.12032.

47. Hülagü, R., and Timur, Ş. (2024). Using Morphological Chart for Analysing Existing Designs, *Archives of Design Research*, Vol. 37, No. 1, 27–41. doi:10.15187/adr.2024.02.37.1.27.

48. Jamea, A., Jing, L., Peng, X., Li, J., and Jiang, S. (2023). Whist Game Cards Calibration Strategies-Based Technique for Conceptual Design Morphological Chart Refinement, *Designs*, Vol. 7, No. 1, 4. doi:10.3390/designs7010004.

49. Rega, S. J., Rohman, T., Ishlah, N. W., and Subekti, S. (2024). Application of the VDI 2221 Method in the Design of an Air-to-Water Converter Device, *JTTM : Jurnal Terapan Teknik Mesin*, Vol. 5, No. 2, 277–288. doi:10.37373/JTTM.V5I2.1126.

50. Guler, K., and Petrisor, D. M. (2021). A Pugh Matrix Based Product Development Model for Increased Small Design Team Efficiency, *Cogent Engineering*, Vol. 8, No. 1. doi:10.1080/23311916.2021.1923383.

51. Piasecki, A., Hożejowska, S., Masternak-Janus, A., and Piasecka, M. (2024). Using Quality Function Deployment to Assess the Efficiency of Mini-Channel Heat Exchangers, *Energies*, Vol. 17, No. 10, 2436. doi:10.3390/en17102436.

52. Previti, A., Brighenti, A., Raynaud, D., and Vezzoni, B. (2023). Towards a Systematic Requirement-Based Approach to Build a Neutronics Study Platform, *Nuclear Science and Engineering*, Vol. 197, No. 9, 2459–2483. doi:10.1080/00295639.2023.2189535.

53. Strunga, A., Kroulíková, T., Bartuli, E., and Raudenský, M. (2022). Experimental Determination of the Heat Transfer Coefficients of Shell-and-Tube Heat Exchangers with Different Hollow Fiber Arrangements, *Journal of Thermal Analysis and Calorimetry*, Vol. 147, No. 24, 14787–14796. doi:10.1007/s10973-022-11576-1.

54. Syed, Z. (2022). *Multiple Heat Exchanger Cooling System for Automotive Multiple Heat Exchanger Cooling System for Automotive Applications-Design, Mathematical Modeling, and Experimental Applications-Design, Mathematical Modeling, and Experimental Observations Observations*Retrieved from https://open.clemson.edu/all_dissertations/3219/.

55. Wang, J., Zhu, J., Zhao, X., Li, L., and Wang, B. (2023). Research on Expert Group Decision-Making and Conflict Resolution in Complex Engineering Consulting Process, *Journal of Intelligent and Fuzzy Systems*, Vol. 44, No. 1, 889–904. doi:10.3233/JIFS-222099.